

## Antiproliferative Activity of Green Process Synthesized *Epipremnum Aureum* Silver Nanoparticles Against Breast Cancer MCF-7 Cells

Yogita Ale<sup>1\*</sup>, Shilpa Rana<sup>2</sup>, Vikash Jakhmola<sup>3</sup>, Kapil Kumar<sup>4</sup>,  
Ritik Singh Rana<sup>1</sup>, Diksha Rawat<sup>1</sup> and Nidhi Nainwal<sup>1</sup>

<sup>1</sup>Department of Pharmaceutics, Uttaranchal Institute of Pharmaceutical Sciences, Uttaranchal University, Dehradun-248007, Uttarakhand, India.

<sup>2</sup>Department of Pharmacology, Uttaranchal Institute of Pharmaceutical Sciences, Uttaranchal University, Dehradun-248007, Uttarakhand, India.

<sup>3</sup>Department of Pharmaceutical Chemistry, Uttaranchal Institute of Pharmaceutical Sciences, Uttaranchal University, Dehradun-248007, Uttarakhand, India.

<sup>4</sup>Samrat Prithviraj Chauhan College of Pharmacy, Kashipur, Uttarakhand Technical University, Uttarakhand, India.

\*Corresponding Author E-mail: yogitaale7@gmail.com

<https://dx.doi.org/10.13005/bpj/2984>

(Received: 30 May 2024; accepted: 18 September 2024)

Breast cancer (BC) is one of the most severe cancers among women globally. Local recurrence of cancer after surgery is usually seen as a poor predictor of prognosis. Cancer treatment has been significantly transformed by the progress made in nanotechnology, and nanoparticles have emerged as pivotal components in this domain. Metal nanoparticles are produced using plant extract in green synthesis or eco-friendly techniques for the stabilizing and reducing substance. The current research study synthesizes silver nanoparticles (AgNPs) from *Epipremnum aureum* leaf extract using the green synthesis method and its evaluations using UV-Vis, FTIR, XRD, SEM, and EDX characterization techniques. The EA-AgNPs exhibit a significant absorption peak at wavelength 420 nm, which confirms the AgNP's presence by UV-visible spectrometer. FTIR spectrum reveals the strong band at 1586.020 cm<sup>-1</sup> confirming the O-H group presence. The stretching and bending modes of vibration of the NO<sub>3</sub><sup>-</sup> a sharp band represented molecule at 1382.987 cm<sup>-1</sup> and a very tiny band at 1272.241, 1077.355 cm<sup>-1</sup>. The XRD spectrum exclusively showed Ag peaks, with no additional chemical contaminants, signifying the sample's purity, and the average particle size was 12.92 nm. MTT assay result observed high cytotoxic activity of EA-AgNPs against MCF-7 cells with IC<sub>50</sub> = 0.1106 μg/ml. This research study aims to preliminary investigate the in-vitro antiproliferative activity of green process synthesized *Epipremnum Aureum* silver nanoparticles (EA-AgNPs) against breast cancer cell line (MCF-7).

**Keywords:** Antiproliferative activity; Breast cancer; Green synthesis; MTT Assay; Silver nanoparticles.

---

Globally, breast cancer (BC) is the primary cause of cancer-associated mortality in women. Based on molecular markers for Human Epidermal Growth factor 2 (ERBB2) and estrogen receptors

(ER), it is divided into three primary subtypes: ER-positive/ERBB2 negative (representing 70% of patients), ERBB2 positive (15–20%), and triple-negative (15%)<sup>1,2</sup>. Chemoresistance induced

by chemotherapy has become one of the most significant causes of chemotherapy failure and has been reported to increase frequently<sup>3</sup>. Recurrence is anticipated to occur in 40% of breast cancer patients, with the largest risk occurring within 1-3 years of reconstruction<sup>1,2</sup>. As a result, a potential treatment that targets specific cancer cells is necessary. However, traditional chemotherapeutic treatments are non-target specific, induce side effects, and attack any rapidly dividing cell, including healthy ones, producing chronic toxicity. Additional adverse effects include mucositis, thrombocytopenia, and alopecia<sup>3,4</sup>.

The application of nanotechnology has benefited the early diagnosis and management of breast cancer. Various nanomaterials including nanofibers, liposomes, nanoparticles, and nano-capsules have been examined to inhibit breast cancer cell growth, recurrence, and post-chemotherapy metastasis<sup>5</sup>. When compared to other conventional methods, sustainable metal oxide nanoparticle formulations have gained significant interest because of their several advantages, which include simple, easily available, cost-effective, non-toxic, and environmentally friendly<sup>6,7</sup>. Metal nanoparticles synthesized using green synthesis or eco-friendly techniques use different parts of plant extracts such as seeds, leaves, stems, and fruit as reducing agents and stabilizers<sup>8</sup>. Silver nanoparticles (AgNPs) gained popularity in nanomedicine because of their chemical stability and carcinogenic activities. Therefore, the green synthesis of nanoparticles may have benefits for therapeutic applications<sup>8</sup>. Prior research has demonstrated that AgNPs operate through the disruption of the mitochondrial electron transfer chain, producing reactive oxygen species (ROS), damage to DNA, and interruption of ATP synthesis. The toxicity of AgNPs is significantly influenced by the overproduction of reactive oxygen species (ROS), as cancer cells are more vulnerable to elevated ROS concentrations compared to healthy cells. Thus, through the elevation of ROS levels, anticancer drugs can trigger apoptosis in tumour cells. Through the Akt/PI3K pathway, AgNPs inhibit VEGF-induced cell proliferation, survival, and migration. Moreover, cancer cells are more vulnerable to the deleterious impacts of silver nanoparticles (AgNPs) in comparison to healthy cells<sup>9,10</sup>.

The current study explored the application of *Epipremnum Aureum* (EA) leaves extract as a green chemistry method for fabricating AgNPs, where *E. aureum* leaves serve as both a reducing and stabilizing agent and were thoroughly characterized. *E. aureum*, a member of the *Araceae* family, is most often known as the Money Plant<sup>11,12</sup>.

Various research findings have revealed that *E. aureum* plant extract or its other species possess various pharmacological activities including anti-inflammatory, anti-cataract, anti-cancer activities, etc. Table 1. represents the pharmacological activity of *E. aureum* plant extract. A research study by Srivastava and his co-workers revealed that the *E. pinnatum* chloroform extract showed significant inhibitory activity against T-47D carcinoma cells. The cell mortality mechanism indicates non-apoptotic and apoptotic cell mortality<sup>13</sup>.

In another study, *E. aureum* leaf extracts were evaluated for antioxidant and antiproliferative effects on MCF-7 and HepG2 cancer cells. Studies found that DPPH radicle scavenging was more effective than ABTS by  $57.2 \pm 2.1$   $\mu\text{g/ml}$ , FRAP, metal chelating value, and hydrogen peroxide was  $51.6 \pm 3.4$   $\mu\text{g/ml}$ ,  $60.4 \pm 1.9$   $\mu\text{g/ml}$ ,  $49.6 \pm 2.7$   $\mu\text{g/ml}$  respectively. The IC<sub>50</sub> values for HepG-2 and breast cancer cells was found to be 41.2  $\mu\text{g/ml}$  and 35.1  $\mu\text{g/ml}$  respectively than tamoxifen standard anticancer drug 12.8  $\mu\text{g/ml}$ <sup>14</sup>. On the basis of various research finding, it was found that *Epipremnum Aureum* (EA) extract possesses different medicinal properties. Therefore, few novel formulations were also synthesized using *E. Aureum* extract, as mentioned in table 2.

The characteristics of silver nanoparticles have led to an increased demand for them in recent years, particularly in the fields of nanotechnology and medicine. However, the safety worries about silver nanoparticles are still not well understood and need more research.

## MATERIALS AND METHODS

### Plant collection and Extraction

#### Preparation of crude drug

Fresh leaves of *Epipremnum Aureum*, were collected from local areas and authenticated by the Botanical Survey of India, Uttarakhand with accession no. 1304. Collected leaves were washed

thoroughly with normal water and distilled water to clear unwanted foreign impurities. Leaves were dried in proper sunlight for 5-6 days. The dried leaves with the help of a mechanical grinder were coarsely powdered<sup>14</sup>.

#### Method of Extraction

For extraction of *Epipremnum Aureum* crude, a soxhlation method using the Soxhlet apparatus was employed. The extraction was carried out using methanol solvent. The 50 gm of *E. Aureum* coarsely dried crude drug was extracted with 250 ml of methanol until the extraction was completed. After the extraction process was completed, the extra solvent was evaporated using a Rotary evaporator at a temperature not exceeding 60°C. A dark greenish color residue was obtained. The residue was allowed to dry and stored in a desiccator. After drying, the percentage yield of the extract was calculated<sup>14</sup>.

#### Green synthesis of Silver nanoparticle of *Epipremnum Aureum*

The silver nanoparticles of *E. Aureum* are prepared using the green synthesis method and a slight modification of the Barik A., (2010) method<sup>15</sup>. In a conical flask, add 100 ml silver nitrate (1 M) and 5gm of plant extract. Mixed the above solution thoroughly using a magnetic

stirrer at 800 rpm for 1.5 hours and also wrapped the above solution with aluminum foil to avoid loss of solvent. To stabilize the prepared silver nanoparticles and eliminate unwanted nitrate ions, 10 ml Sodium Hydroxide solution (1 M) was added dropwise with continuous stirring for the next 30 min. After the addition of NaOH, the solution turned dark brown to black, indicating the development of EA-AgNPs. The whole process was performed in a dark room at room temperature to avoid photoactivation of AgNO<sub>3</sub>. Suitable parameters were maintained throughout the experiment<sup>14</sup>. After the above process, the mixture was cooled at room temperature and followed by a centrifugation process at 1500 rpm for 3 min. The resulting black-colored AgNPs were settled at the centrifuge tube bottom and the supernatant layer was discarded. The prepared NPs were washed with distilled water, and the above procedures were repeated until EA-AgNPs were collected and washed. The collected EA-AgNPs were firstly dried at room temperature and further calcinated at a temperature of 250°C for 2 hours to remove any impurities, water, or excess solvents. The schematic representation of the whole process is shown in figure 1. Finally, the prepared EA-AgNPs were preserved for further characterization process<sup>16,17</sup>.

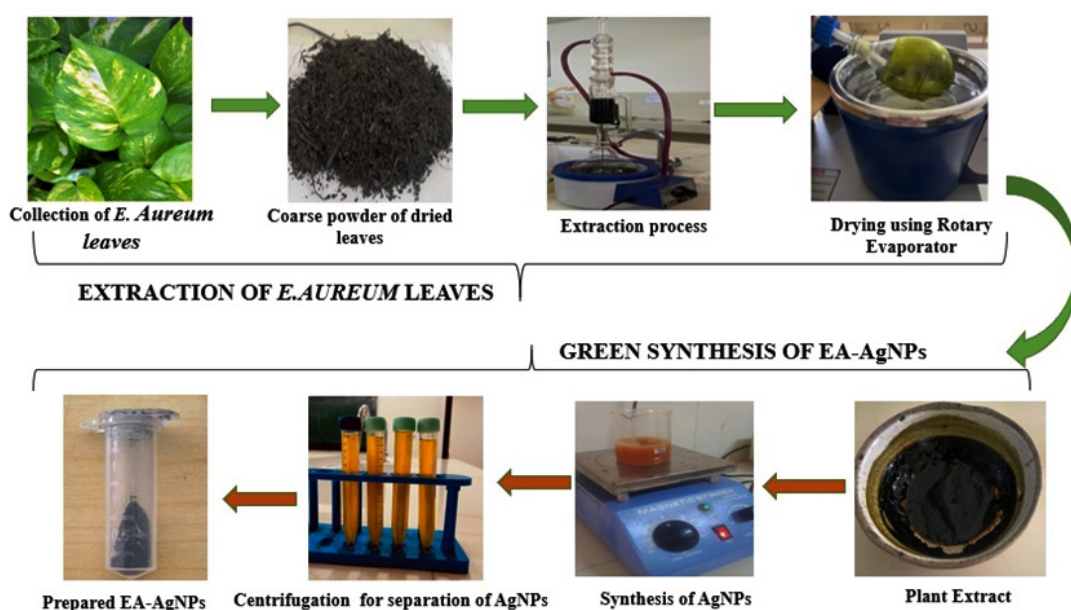


Fig. 1. Schematic representation of extraction and green synthesis of EA-AgNPs

Table 1. Tabular representation of *Epipremnum aureum* plant extract used in various Pharmacological activity

Plant Species and Extract	Part used	Plant Species Authentication	Activity	Study Model	Key finding	References
<i>Epipremnum aureum</i> Chloroform and ethanol extracts	Leaves	Authenticated by BSI, Pune (BSI/WRC/100-1/Tech./2020/117).	Anticancer activity for breast cancer	In-vitro Study (Cytotoxicity study on MCF-7 cell line)	Results indicated cytotoxic effects with IC50 values of 32.9 and 45.8 ig/mL for chloroform and ethanolic, respectively. Microscopic inspection reveals apoptotic entities, nuclear disintegration, and small nuclei with significant chromatin condensation in the extract.	24
<i>Epipremnum aureum</i> Ethanolic extract	Leaves	Department of Botany, University of Calicut, itself. (Specimen 148207)	Anticancer activity Dalton's Ascitic Lymphoma	In-vitro study (DAL cell line) and In-vivo study Animal use: Swiss Albino mice	In the MTT assay, EEEA showed an IC50 value of 140.95 µg/ml. In the Trypan blue dye exclusion experiment, EEEA has an IC50 of 158.89µg/ml. In-vivo study indicated EEEA increased mice lifespan and reduced body weight, tumour volume, tumour weight, and viable cell count compared to untreated DAL control animals.	25
<i>Epipremnum aureum</i> Ethanolic extracts	Leaves	Maharani College, Peddapuram, and voucher specimen number given is 23113.	Anti-oxidant and Anti-cataract activity	In-vitro anticataract activity. Galactose model in animals.	DPPH radical scavenging results indicate concentration-dependent antioxidant activity, with an IC50 of 87.09 µg/ml. The IC50 was 24.5 µg/ml in the nitric oxide scavenging assay. In-vitro and in-vivo studies show reduced cataract lens opacity.	26
<i>Epipremnum aureum</i> Ethanolic and acetone extracts	leaves blades, petioles, stems, and roots	Herbarium of Botany and Microbiology Department, Cairo University, Giza, Egypt.	Antimicrobial activity and Anti-cancer activity.	In-vitro Antimicrobial activity. In-vitro cytotoxicity activity human liver cancer cell line (HEPG-2)	The root extracted with acetone was shown to be the most effective antibacterial extract. <i>E. aureum</i> acetone root extract had MIC values of 3, 5, and 9 mg/ml for <i>E. coli</i> , <i>S. aureus</i> , and <i>C. albicans</i> . In vitro, cytotoxicity testing of <i>E. aureum</i> acetone root extract against HEPG-2 human liver cancer cells revealed the most effective concentration at 50 ig/ml, with an IC50 value of 36.7 ig/ml.	27
<i>Epipremnum aureum</i> Ethanolic extract	Whole plant	Forest Research Institute Malaysia. The voucher specimen (No. SBID: 001/15)	Anti-Amnesic Activity	In-vivo Swiss albino mice	Results indicated dose-dependent memory enhancement and scopolamine amnesia reversal. Biochemical analysis indicates a rise in acetylcholine and a decrease in TBARS, reversing the impact of scopolamine in amnesic mice.	28
<i>Epipremnum aureum</i> Ethanolic extract	leaves	Forest Research Institute Malaysia. The voucher specimen (No. SBID: 001/15)	Acute and sub chronic toxicity studies	In-vivo study (Adult Sprague Dawley rats)	Acute oral Epipremnum aureum administration did not cause death or CNS/ANS toxicity. Similarly, in subchronic toxicity trials, Epipremnum aureum showed no obvious evidence of toxicity. No treatment-related histopathological alterations were found	29
<i>Epipremnum aureum</i> Methanolic extract	leaf, root and stem)	Botanical Survey of India, Jodhpur	Anti-oxidant activity (enzymes catalase, glutathione peroxidase and	In-vitro study DPPH and FRAP methods.	The catalase and peroxidase enzymes in the leaves exhibited a high antioxidant activity. The highest IC50 value was found in <i>E. aureum</i>	30

<i>Epipremnum aureum</i> Aqueous and methanolic extracts	leaves	Head of Botany Dept, YC Mahavidyalay, Warananagar, Affiliated to Shivaji University, Kolhapur.	superoxide dismutase) Antioxidant activity DPPH radical scavenging activity assay, total reduction capacity assay and FRAP assay.	In-vitro test	stems, while leaves had the highest free radical scavenging potential. The concentration-dependent antioxidant activity of DPPH radical scavenging was shown to have an IC50 of 100 µg/ml. Total phenolic content was 852.379 mg/ml aqueous GAE extract and 559.522 mg/ml GAE alone. It was found that the FRAP values of the methanolic and aqueous extracts were, respectively, 1.716 and 1.932.	31
<i>Epipremnum aureum</i> Ethanollic extract	leaves	Voucher specimen (GPS 30.967561, 76.519004) verified by Dr. A.S. Sandhu, National Institute of Pharmaceutical Education and Research (NIPER)	Neuroprotective Activity against Rotenone-induced neurotoxicity.	In-vivo study Wistar rats	ROT-treated rats had higher catatonic and paw retraction times and lower ambulatory and rearing scores. Rotenone-induced motor symptoms were markedly reversed in mice treated with EEA (250 and 500 mg/kg). Significantly reduced intranigral ROT-induced brain TBARS, GSH, and catalase activity.	32
<i>Epipremnum aureum</i> Chloroform extract	leaves	Botanical Survey of India, Jodhpur.	Anti-termite Assay	In-vitro test	The findings revealed a moderate level of termiticidal activity that gradually rose over time, from 19.33% to 24.33%.	33

**Table 2.** Tabular presentation of different novel formulations prepared using *Epipremnum aureum* plant extract

Plant Species and Extract Used	Extraction process	Formulations	Method of preparation	Study	Key findings	References
<i>Epipremnum aureum</i> Aqueous extract	Digestion method	Zinc Oxide Nanoparticles ZnO-NPs	Green Biological method	To study photocatalytic degradation of Congo red using ZnO NPs	The current investigation found optimum photocatalytic degradation at 10 ppm, pH (2), 20 mg catalyst, and 100 min contact duration. Results showed Langmuir isotherm fitting best, followed by Freundlich, Temkin, and Elovich isotherms.	34
<i>Epipremnum aureum</i> Aqueous extract	Digestion method	Zinc Oxide Nanoparticles Silver Nanoparticles (ZnO-NPs and AgNPs)	Green Biological method	Characterization of prepared NPs.	Various characterization analysis was conducted (SEM, AFM, FTIR etc.) which showed satisfactory results.	35
<i>Epipremnum aureum</i> Aqueous extract	Digestion method	Zinc Oxide Nanoparticles Silver Nanoparticles (ZnO-NPs and AgNPs)	Green Biological method	PA-1 cell line (Ovarian Cancer)	<i>E. aureum</i> ZnO nanoparticles had an IC50 of 16.487, compared to Cisplatin's 2.728.	36

### Characterization of EA-Silver nanoparticle Percentage Yield

The percentage of yield of the *E. Aureum* plant extract after extraction is calculated after the drying process using the formula below formula.

$$\text{Percentage Yield} = (\text{Weight of extract} \div \text{Weight of dried plant material}) \times 100$$

### UV Spectroscopy

The silver ion bioreduction process was facilitated by the initial transition in color from

green to silvery brown-black. Additionally, it was confirmed by comparable peaks seen in the EP-AgNPs solution's spectrum using a Shimadzu UV double-beam spectrophotometer (model 1900i). The operational wavelength range was 200–1000 nm<sup>16,17</sup>.

### XED Analysis

The X-ray powder diffraction technique was employed to determine the crystallinity of biogenic EA-AgNPs. A scan was captured at an angle of 2θ and a temperature range of 30° to 80°C<sup>18</sup>.

### FTIR Analysis

To examine the existence of functional groups in biogenic EA-AgNPs, FTIR analysis was used. The KBr pellet method was used for the measurements, with relevant spectrum scans ranging from 500 to 4000  $\text{cm}^{-1}$  (Nicolet Summit LITE spectrometer)<sup>18</sup>.

### SEM-EDX Analysis

To study the structure and shape, SEM and EDX analysis was conducted. Dried biogenic EA-AgNPs were prepared on a copper-coated carbon grid and observed using a scanning electron microscope (Carl Zeiss EVO18) to determine their form and bonding configuration. The EDX study was used to determine elements present in the biogenic EA-AgNPs. Cu-K $\alpha$  radiation was utilized to perform the scan within the 2 $\theta$  range of 10 to 80 $^\circ$ , with an applied voltage of 40 kV and an amperage of 35 mA<sup>18</sup>.

### In-Vitro cytotoxicity study

The MTT test used to evaluate the antiproliferative activity of EA-AgNPs samples on the MCF-7 cells which was obtained from NCCS Pune. In 96-well plates, 10,000 cells were cultured with 5% CO<sub>2</sub> in Dulbecco's modified eagle medium (DMEM) along with 10% fetal bovine serum (FBS) and 1% antibiotic solution for 24 hours at 37 $^\circ\text{C}$ . The cultured cells were exposed to varying concentrations of prepared EA-AgNPs, i.e., 1  $\mu\text{g}/\text{ml}$ , 10  $\mu\text{g}/\text{ml}$ , 50  $\mu\text{g}/\text{ml}$ , 100  $\mu\text{g}/\text{ml}$ , 250  $\mu\text{g}/\text{ml}$ , 500  $\mu\text{g}/\text{ml}$  and 1000  $\mu\text{g}/\text{ml}$ . The untreated cultured cells were used as controls. After 24 hours of incubation, the cell culture was mixed with the prepared 250  $\mu\text{g}/\text{ml}$  of MTT solution and incubated for the next 2 hours. On completion of the above process, the supernatant layer of the cultured medium was collected, and the cell

**Table 3.** EA-AgNPs size was determined using the Debye Scherrer equation

Peak Position (2 Theta)	FWHM	Crystalline Size D (nm)	D nm (Average)
29.75	0.42208	18.19	12.92
38.27	0.41201	18.21	
44.44	0.4446	16.54	
64.62	182.6407	0.03	
77.54	0.53204	11.64	

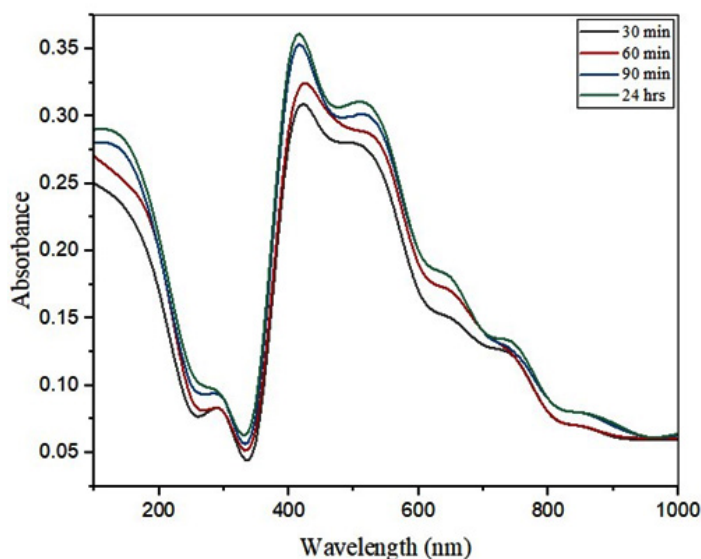


**Fig. 2.** The UV-visible absorption spectrum of EA-AgNPs

matrix layer was dissolved in 100  $\mu$ l of Dimethyl Sulfoxide (DMSO) and observed in an Elisa plate reader (iMark, Biorad, USA) at 540 and 660 nm. Using Graph Pad Prism-6 software the IC-50 value was determined. The images of cell culture treated and controlled cell cultured were taken using an inverted microscope (made: Olympus ek2) with the camera (made: Amscope digital camera 10MP Aptima CMOS)<sup>18-21</sup>.

## RESULTS AND DISCUSSION

### Percentage Yield

The 50 gm of *E. Aureum* coarsely dried crude leaves showed a percentage yield of 20% with methanol solvent (250 ml) using the soxhlation method.

### UV Spectroscopy

The addition of leaf extracts into an aqueous silver nitrate solution resulted in a

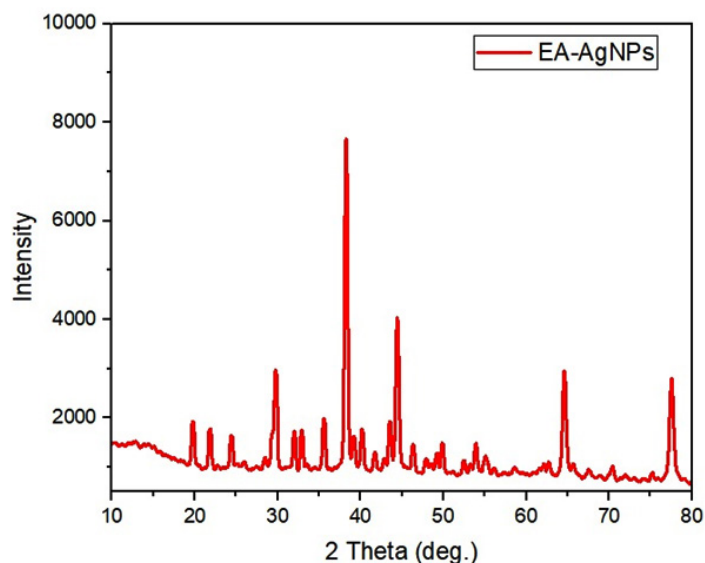


Fig. 3. XRD of EA-AgNPs

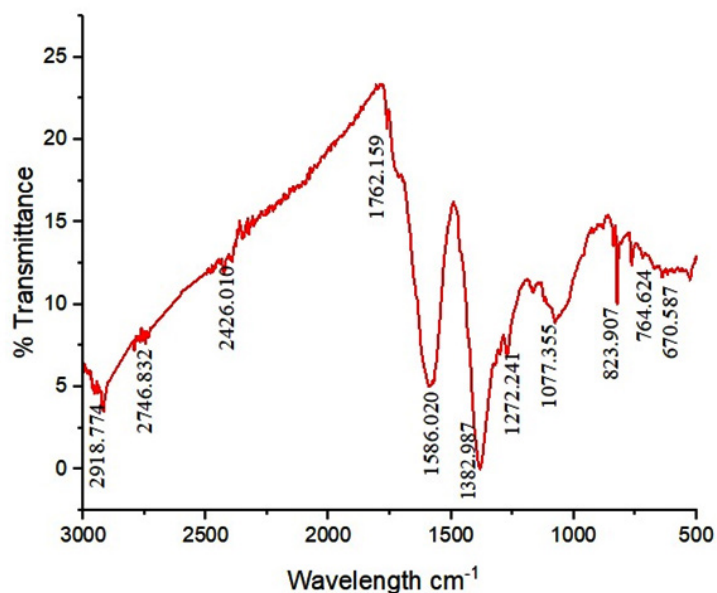


Fig. 4. FTIR Spectrum of EA-AgNPs

color transition from pale light to yellowish brown, and colloidal brown, indicating the formation of AgNPs. The color transition is the result of the surface plasmon vibration. In this study, a similar color change has been observed confirming the reaction occurred between leaf extract and AgNO<sub>3</sub> completed. The UV-visible spectroscopy at wavelength 200–1000 nm was used to analyze the formation of EA-AgNPs. The UV-visible spectrum was observed in time intervals of 30, 60, 90 minutes and 24 hours from the initiation of the reaction are shown in Figure 2. The results revealed the formation of spectral absorption peaks for Ag from *Epipremnum Aureum* leaves NPs. The EA-AgNPs exhibit a significant absorption peak at 420 nm, confirming AgNPs presence in the solution since the absorption peaks at wavelengths

400–450 nm range are the characteristic properties of AgNPs due to Surface Plasmon Resonance (SPR). The UV-visible spectrum absorbs the bulk of SPPR, determining the bio-reduction process of Ag<sup>+</sup> and the size and shape of NPs by determining absorptive locations at wavelengths that increase NP size and shift the SPPR peak to a longer wavelength<sup>18–21</sup>.

#### XRD study

#### Crystallographic analysis of OS-AgNPs

The XRD results reveal the size and crystalline phase of biogenic EA-AgNPs. The EA-AgNPs diffraction peaks at positions 29.75, 38.27, 44.44, 64.62, and 77.54 confirm that the corresponding Bragg reflections are (100), (112), (200), (219), and (315), respectively (Fig. 3). The cubic face-centered shape of the synthesized

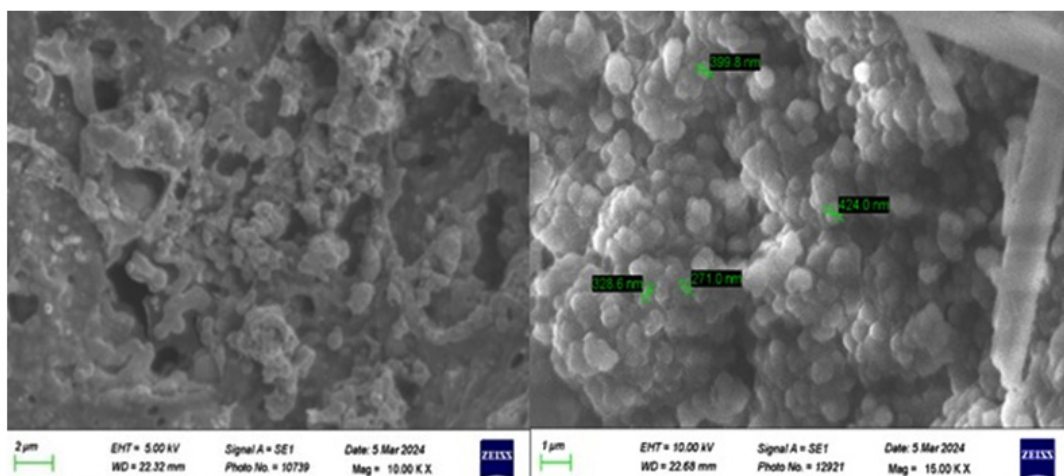


Fig. 5. SEM images of EA-AgNPs

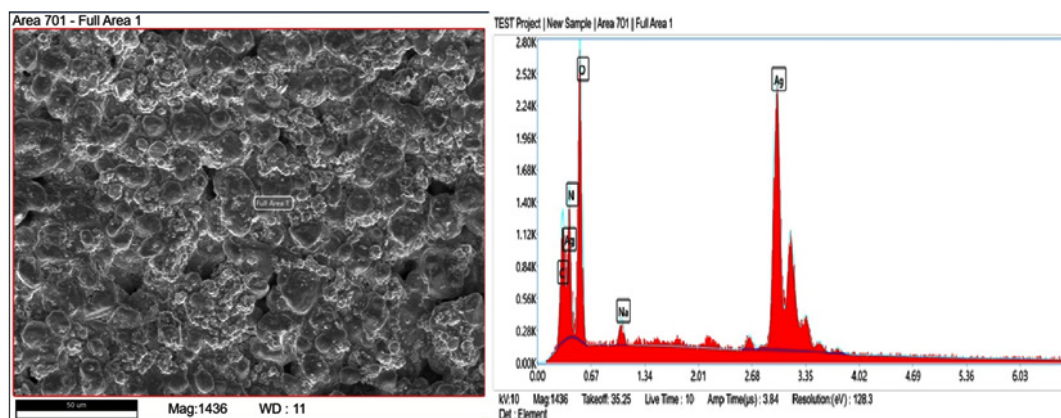


Fig. 6. EDX Results of EA-AgNPs



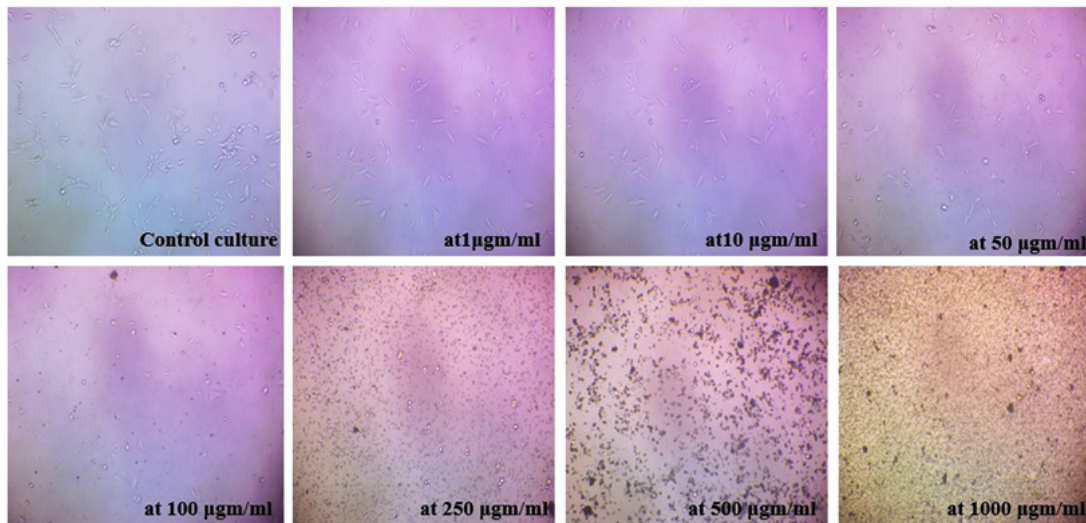


Fig. 7. MTT Assay images MCF-7 cells exposed to EA-AgNPs in various concentrations for 24 hrs

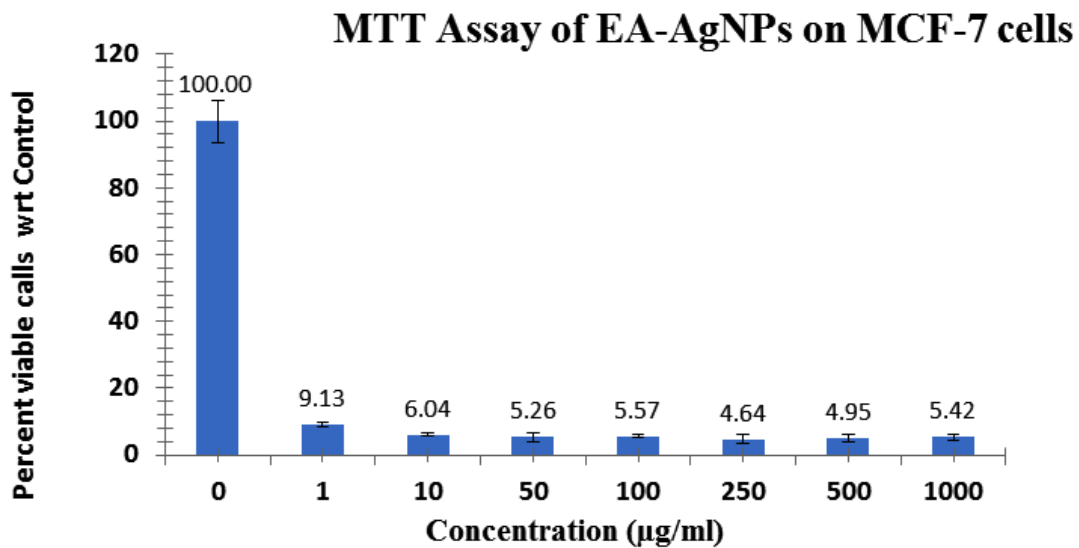


Fig. 8. MTT assay of synthesized EA-AgNPs against MCF-7 cell line

EA-AgNPs was verified by hkl values. Debye Scherrer’s formula was applied to evaluate the particle size of the EA-AgNPs:

$$D = \frac{k\lambda}{\Delta 2\cos\theta} \times 100$$

Where, k = geometric factor’s shaped constant,

$\lambda$  = wavelength,

$\Delta$  = line broadening at half-maximum amplitude

$\theta$  = Bragg angle,

D = average crystalline size of the NPs.

Low particle size and high crystallinity are indicated by the extreme peak positions. Using Origin software and the Scherrer formula, the average particle size of EA-AgNPs was 12.92 nm as shown in Table 3

The XRD spectrum exclusively showed Ag peaks, with no additional chemical contaminants, further demonstrating the sample’s purity.

### FTIR Study

The primary functional group implicated in EA-AgNPs synthesis was identified via an analysis of the FTIR spectra of biogenic EA-AgNPs. The EA-AgNPs spectra revealed the characteristic groups involved in stabilizing EA-AgNPs by an absorption peak found at 1382.987, 1586.020, 1762.159, 1272.241, 1077.355, 823.907, 764.624, and 670.587  $\text{cm}^{-1}$  (Fig. 4). A strong band at 1586.020  $\text{cm}^{-1}$  confirmed the O-H group presence. The stretching and bending modes of vibration of the  $\text{NO}_3^{2-}$  a sharp band represented molecule at 1382.987  $\text{cm}^{-1}$  and a very tiny band at 1272.241, 1077.355  $\text{cm}^{-1}$ . The spectrum of silver metal can be seen in the narrow shallow band at 670.587  $\text{cm}^{-118}$ .

### SEM-EDX Study

The shape of the EA-AgNPs was established by the surface topography, which was observed through SEM. The well-defined spherical and irregular morphologies of the synthesized EA-AgNPs were observed (Fig. 5). Similar structures of AgNPs range of sizes and shapes using *Artemisia nilagirica*. Additionally, these NPs were investigated for their pupicidal and larvicidal effects in *Anopheles stephensi* and *Aegypti*<sup>22,23</sup>.

EDX examination demonstrates the weight percentage of the  $\text{Ag}^+$  ions (29.3%), confirming the EA-AgNPs formations as shown in Figure 6.

### EP-AgNPs' *In Vitro* Cytotoxicity against MCF-7 Cell Line

After incubation for 24 hours, an inhibitory effect was observed (Figure 7). The graph was plotted against percentage control on the y-axis with different concentrations of EA-AgNPs (1, 10, 50, 100, 250, 500, and 1000  $\text{ig/mL}$ ) on the x-axis as shown in Figure 8. The 100% cell viability was observed when cells cultured were untreated with EA-AgNPs. On exposure to varying concentrations of EA-AgNPs samples i.e., 1, 10, 50, 100, 250, 500, and 1000  $\text{ig/mL}$  resulted in the following percentages relative to the control: 9.13, 6.04, 5.26, 5.57, 4.64, 4.95, and 5.42, respectively. Based on the results of the MTT experiment, the half-maximal inhibitory concentration ( $\text{IC}_{50}$ ) values obtained for EA-AgNPs against MCF-7 cells were found to be 0.1106  $\text{ig/mL}$ , which shows high cytotoxic behavior of EA-AgNPs against MCF-7 cells.

### CONCLUSION

Plant extract-based AgNPs approach provided a promising avenue for treating drug resistance and minimizing the harmful effects associated with chemotherapy treatments. In the current study, synthesized EA-AgNPs showed potential cytotoxicity on MCF-7 breast cancer cells. The characterization techniques including UV-visible spectrophotometry, XRD, FTIR, and EDX analysis confirmed the formation of EA-AgNPs. The in-vitro MTT assay results demonstrated the antiproliferative activity of EA-AgNPs with high cytotoxic efficacy against MCF-7 breast cancer cells. According to these finding the biosynthesized EA-AgNPs have the potential to be utilised as a rapid, simple, cost-effective, and environmentally benign treatment for the fatal disease breast cancer. Still, more investigation is needed to fully understand the underlying mechanism.

### ACKNOWLEDGEMENT

The authors would like to show gratitude to Mr. Jitender Joshi, (President), and Prof. (Dr.) Dharam Buddhi, (Vice Chancellor), Uttarakhand University, for their support. We are thankful to Research and Innovation (DRI) and the Central Instrumentation Facility (CIF) of Uttarakhand University Dehradun, for providing the facilities needed for the research experiment.

### Conflict of Interest

The authors do not have any conflict of interest.

### Funding Sources

This research study is executed under the seed money project, funded by the Division of Research and Innovation (DRI), Uttarakhand University Dehradun (India), the grant number of funding sources is UU/DRI/SM/2022-23/005.

### Data Availability Statement

The manuscript incorporates all datasets produced or examined throughout this research study.

### Ethics Statement

This research did not involve human participants, animal subjects, or any material that requires ethical approval.

### Informed Consent Statement

This study did not involve human

participants, and therefore, informed consent was not required.

#### Authors Contribution

Y.A (Yogita Ale): Conceptualization, Methodology, Analysis, Writing – Original Draft.; S.R (Shilpa Rana): Data Collection, Analysis, Writing – Review & Editing.; V.J (Vikash Jakhmola): Visualization, Supervision, Project Administration.; K.K (Kapil Kumar): Funding Acquisition, Resources, Supervision.; R.S.R (Ritik Singh Rana): Analysis and data collection.; D.R (Diksha Rawat): Analysis and data collection.; N.N (Nidhi Nainwal): Visualization, Supervision, Project Administration.

#### REFERENCES

1. Alshareeda A.T., Nur Khatijah M.Z., Al-Sowayan B.S. Nanotechnology: A revolutionary approach to prevent breast cancer recurrence. *Asian J Surg.* 2023;46(1):13-17.
2. Zhang Y.N., Xia K.R., Li C.Y., Wei B.L., Zhang B. Review of Breast Cancer Pathological Image Processing. *Biomed Research International* 2021;2021(1):01-7.
3. Sonavane A.B., Shinde A.R., Raut N.T. Review Article on Breast Cancer. *Int J Res Appl Sci Eng Technol.* 2024;12(3): 679-684.
4. Warriar S., Tapia G., Goltsman D., Beith J. An update in breast cancer screening and management. *Women's Health.* 2016;12(2):229-239.
5. Tao L., Chen X., Sun J., Wu C. Silver nanoparticles achieve cytotoxicity against breast cancer by regulating long-chain noncoding RNA XLOC\_006390-mediated pathway. *Toxicol Res (Camb).* 2021;10(1):123-133.
6. Zhang X.F., Liu Z.G., Shen W., Gurunathan S. Silver nanoparticles: Synthesis, characterization, properties, applications, and therapeutic approaches. *Int J Mol Sci.* 2016;17(9):1534.
7. Roy A., Bulut O., Some S., Mandal A.K., Yilmaz M.D. Green synthesis of silver nanoparticles: Biomolecule-nanoparticle organizations targeting antimicrobial activity. *RSC Adv.* 2019;9(5):2673-2702.
8. Tuli H.S., Joshi R., Kaur G., Garg V.K., Sak K., Varol M., Kaur J., Alharbi S.A., AlAHMADI t.a., Diwakar A., Dhama K., Jaswal V.S., Mittal S., Sethi G. Metal nanoparticles in cancer: from synthesis and metabolism to cellular interactions. *J Nanostructure Chem.* 2023;13(3):321-348.
9. Kuppusamy P., Yusoff M.M., Maniam G.P., Govindan N. Biosynthesis of metallic nanoparticles using plant derivatives and their new avenues in pharmacological applications – An updated report. *Saudi Pharmaceutical Journal.* 2016;24(4):473-84.
10. Zahoor M., Nazir N., Iftikhar M., Naz S., Zekker I., Burlakovs J., Uddin F., Kamran A.W., Kallistova A., Pimenov N.V., Khan F.A. A review on silver nanoparticles: Classification, various methods of synthesis, and their potential roles in biomedical applications and water treatment. *Water (Switzerland).* 2021;13(16):2216.
11. Panchal V., Sapra P., Mankad A. Bio Efficacy Of Epipremnum Aureum: A Review. *International Association of Biologicals and Computational Digest.* 2022;1(2):59-63.
12. Patil S.S., Wadkar K.A. In vitro anti-cancer activity of Epipremnum aureum. *Bangladesh J Pharmacol.* 2024;19(1):23-28.
13. Shwarupa S., Suresh Bhagyawant S., Srivastava N. Comparative Study on the Anti-Termite, Antimicrobial and Antioxidant Activity of Leaf and Root Extracts of Pothos Aurea (Epipremnum aureum L.). *Journal of Pharmaceutical Research & Clinical Practice.* 2011;1(2).
14. Gupta N., Meshram A., Khaera A., Srivastava N. Bhagyawanta S.S.. Phytochemical, antioxidant and anti-proliferative activity of Epipremnum aureum. *Afr J Biotechnol.* Published online 2024.
15. Roy N., Barik A. Green Synthesis of Silver Nanoparticles from the Unexploited Weed Resources. *Int J Nanotechnol Appl.* 2010;4(2): 95-101.
16. Hammodi H.F., Rashid I.H., Oraibi A.G. Green biosynthesis, identification and characterization of ag and zn nanoparticles using ivy (*Epipremnum aureum*) plant extract. *Plant Arch.* 2019;19:959-965.
17. Zhang T., Qi M., Wu Q., Xiang P., Tang D., Li Q. Recent research progress on the synthesis and biological effects of selenium nanoparticles. *Front Nutr.* 2023;10:1-12.
18. Ahmed R.H., Mustafa D.E. Green synthesis of silver nanoparticles mediated by traditionally used medicinal plants in Sudan. *Int Nano Lett.* 2020;10(1): 1-14.
19. Bahuguna A., Khan I., Bajpai V.K., Kang S.C. MTT assay to evaluate the cytotoxic potential of a drug. *Bangladesh J Pharmacol.* 2017;12(2):115-118.
20. Ghasemi M., Turnbull T., Sebastian S. Kempson I. The MTT assay: Utility, limitations, pitfalls, and interpretation in bulk and single-cell analysis. *Int J Mol Sci.* 2021;22(23):12827.
21. Nga N.T.H., Ngoc T.T.B., Trinh N.T.M., Thuoc T.L., Thao D.T.P. Optimization and application of MTT assay in determining density of suspension

- cells. *Anal Biochem.* 2020;610(1-2): 113937.
22. Oves M., Ahmar Rauf M., Aslam M., Qari H.A., Sonbol H., Ahmad I., Zaman G.S., Saeed M. Green synthesis of silver nanoparticles by *Conocarpus Lancifolius* plant extract and their antimicrobial and anticancer activities. *Saudi J Biol Sci.* 2022;29(1): 460-471.
23. Singh H., Du J., Yi T.H. Green and rapid synthesis of silver nanoparticles using *Borago officinalis* leaf extract: anticancer and antibacterial activities. *Artif Cells Nanomed Biotechnol.* 2017;45(7): 1310-1316.
24. Patil S.S., Wadkar K.A. In vitro anti-cancer activity of *Epipremnum aureum*. *Bangladesh J Pharmacol.* 2024;19(1): 23-28.
25. Venkatesh S., Muhamed K. Mridhul M.P., Asheena A.V.V., Anjitha P., Suresh A. M Anti-Tumor and Anti-Oxidant Activity of Ethanolic Extract of *Epipremnum aureum* Linn. Leaves against DAL Induced Tumor in Swiss Albino Mice. *International Journal of Current Science Research and Review.* 2021;04(08): 1008-1021.
26. Ramya K., Shaik T., Ramesh B., Ravi Shankar K. Antioxidant and anti-cataract activity of ethanolic extract of *Epipremnum aureum* leaves: In vitro and in vivo study. *Asian J Pharm Pharmacol.* 2023;9(3): 70-77.
27. Ali E. Antimicrobial activity, cytotoxicity and phytochemicals screenings of *Epipremnum aureum* (Linden and Andre) G. S. Bunting extracts. *The Egyptian Journal Of Experimental Biology (Botany).* 2018;14(2): 219-225.
28. Das S.K., Chakraborty G.S., Chakrabarti T., Charkrabarti P., Mohammad N., Mohammad J. Evaluation of nootropic activity of standardized *Epipremnum aureum* extract against scopolamine-induced amnesia in experimental animals. *Journal of Advanced Medical Sciences and Applied Technologies.* 2021;6(1):64-71.
29. Das S.K., Sengupta P., Mustapha M.S., Das A., Sarker M.M.R., Kifayatullah M. Toxicological investigation of ethanolic extract of *Epipremnum aureum* in rodents. *J Appl Pharm Sci.* 2015;5(2): 57-61.
30. Meshram A., Srivastava N. Phytochemical screening and in vitro antioxidant potential of methanolic extract of *Epipremnum aureum* (Linden and Andre) G. S. Bunting. *International Journal of Pharmaceutical Research & Allied Sciences.* 2016;5(2):01-06.
31. Sherikar A.S., Mahanthes M.C. Evaluation of aqueous and methanolic extract of leaves of *Epipremnum aureum* for radical scavenging activity by DPPH Method, total phenolic content, reducing capacity assay and FRAP assay. *J Pharmacogn Phytochem.* 2015;4(4):36-40.
32. Sood S., Kumar M., Bansal N. Ethanol extract of *Epipremnum aureum* leaves attenuate intranigralrotenone induced Parkinson's disease in rats. *Journal of Pharmacy & Pharmacognosy Research.* 2020;8(3):225-236.
33. Meshram A., Singhal G., Bhagyawani S.S., Srivastava N. Characterization of bioactives in chloroform extract of *Epipremnum aureum* leaves using spectroscopy for its antitermite effect. *International journal of basic and applied research.* 2018;8:55-68.
34. Brishti R.S., Ahsan Habib M., Ara M.H., Karim K.M.R., Islam M.K., Naime J., Rumon M.M.H., Khan M.A.R. Green synthesis of ZnO NPs using aqueous extract of *Epipremnum aureum* leave: Photocatalytic degradation of Congo red. *Results Chem.* 2024;7.101441.
35. Hammodi H.F., Rashid I.H., Oraibi A.G. Green biosynthesis, identification and characterization of ag and zn nanoparticles using ivy (*Epipremnum aureum*) plant extract. *Plant Arch.* 2019;19:959-965.
36. Sharmila D., Jeyanthi Rebecca L., Hridayanka K. S. N., Rao M.K.R. In vitro anticancer potential of green-synthesized zinc oxide nanoparticles from leaves of *Epipremnum aureum*. *International Conference on Advances in Science and Technology.*